

- [15] R. Annavajjala, P. C. Cosman, and L. B. Milstein, "On the performance of optimum noncoherent amplify-and-forward reception for cooperative diversity," in *Proc. IEEE MILCOM*, Atlantic City, NJ, Oct. 17–20, 2005, vol. 5, pp. 3280–3288.
- [16] S. M. Kay, *Fundamentals of Statistical Signal Processing: Detection Theory*. Upper Saddle River, NJ: Prentice-Hall, 1993.
- [17] M. R. Souryal, "Non-coherent amplify-and-forward generalized likelihood ratio test receiver," presented at the IEEE GLOBECOM, 2007.
- [18] Y. Zhu, P.-Y. Kam, and Y. Xin, "Non-coherent detection for amplify-and-forward relay systems in a Rayleigh fading environment," in *Proc. IEEE GLOBECOM*, Nov. 2007, pp. 1658–1662.
- [19] Q. Zhao and H. Li, "Performance of differential modulation with wireless relays in Rayleigh fading channels," *IEEE Commun. Lett.*, vol. 9, no. 4, pp. 343–345, Apr. 2005.
- [20] T. Himsoon, W. Su, and K. J. R. Liu, "Differential transmission for amplify-and-forward cooperative communications," *IEEE Signal Process. Lett.*, vol. 12, no. 9, pp. 597–600, Sep. 2005.
- [21] W. Cho and L. Yang, "Distributed differential schemes for cooperative wireless networks," in *Proc. IEEE ICASSP*, May 2006, vol. IV, pp. 61–64.
- [22] T. W. Anderson, *An Introduction to Multivariate Statistical Analysis*, ser. Wiley Series in Probability and Statistics. New York: Wiley, 2003.
- [23] R. Annavajjala, P. C. Cosman, and L. B. Milstein, "Performance analysis of linear modulation schemes with generalized diversity combining on Rayleigh fading channels with noisy channel estimates," *IEEE Trans. Inf. Theory*, vol. 53, no. 12, pp. 4701–4727, Dec. 2007.
- [24] R. Annavajjala, "On Optimum Regenerative Relaying With Imperfect Channel Knowledge, Tech. Rep. [Online]. Available: <http://www.box.net/annavajjala>
- [25] W. R. LePage, *Complex Variables and the Laplace Transform for Engineers*. New York: Dover, Feb. 1980.
- [26] J. G. Proakis, *Digital Communications*, 4th ed. New York: McGraw-Hill, 2001.

## Space–Time Block Coding for Doubly-Selective Channels

Kun Fang and Geert Leus

**Abstract**—In this paper, we present a new space–time block code for time- and frequency-selective (doubly-selective) channels. It can be interpreted as the extension of the Alamouti code to doubly-selective channels, and relies on a joint time–frequency reversal of the transmitted sequences. Under certain channel conditions, the proposed space–time block code belongs to the class that achieves full spatial, delay, and Doppler diversity using a maximum-likelihood (ML) receiver, as well as a linear zero-forcing (LZF) or linear minimum mean-squared error (LMMSE) receiver. For realistic doubly-selective channels, a real-valued linear data model is presented, for which different receiver structures can be developed.

**Index Terms**—Delay diversity, Doppler diversity, doubly-selective channels, space–time block coding.

### I. INTRODUCTION

Broadband wireless communication systems require high transmission rates giving rise to frequency-selectivity due to multipath propagation. On the other hand, recent wireless communication standards

Manuscript received February 05, 2009; accepted October 30, 2009. First published November 24, 2009; current version published February 10, 2010. This work was supported in part by the NWO-STW under the VIDI program (DTC.6577). The associate editor coordinating the review of this manuscript and approving it for publication was Dr. Sergiy A. Vorobyov.

The authors are with the Faculty of Electrical Engineering, Mathematics, and Computer Science (EEMCS), Delft University of Technology, 2628 CD Delft, The Netherlands (e-mail: k.fang@tudelft.nl; g.j.t.leus@tudelft.nl).

Digital Object Identifier 10.1109/TSP.2009.2037349

not only require high rates, but they also need to support high mobile speeds. The high-mobility terminals and scatterers induce Doppler shifts which introduce time-selectivity. Doubly-selective channels can provide multiplicative delay-Doppler diversity gains if the transceiver is properly designed [1], [2]. In the last decade, multi-antenna systems have attracted a lot of research interest for future wireless systems. The use of multiple transmit and/or receive antennas can significantly enhance communication system performances such as channel capacity and reliability [3]. Space–time block coding (STBC) [4], [5] has been introduced to achieve the spatial diversity offered by multiple transmit and/or receive antennas. However, as STBC is typically designed for flat-fading channels, the time- and frequency-selectivity will seriously degrade the system performance. Thus, it is crucial to accurately model the doubly-selective channel and to design efficient STBC schemes to counteract its effects.

Many papers have extended STBC design to frequency-selective channels. In [6], STBC has been proposed for single-carrier transmission, which can achieve maximum space-delay diversity in rich scattering channels. The transmission formats proposed in [6] subsume those of [7], [8], which present time-reversal STBC at the transmitter to achieve transmit diversity. Multicarrier transmission systems have been considered in [9]–[11]. A space–time–multipath coded system is developed in [12] using digital phase sweeping (DPS) in the frequency domain or circular delaying in the time domain, which guarantees the maximum possible space-delay diversity, and has full rate for any number of transmit–receive antennas. Note that the aforementioned algorithms all require the channel to be constant over the entire space–time codeword.

Among the papers considering time-selective channels, [13] designs STBC for purely time-selective channels by transforming the time-selective channels into frequency-selective channels, and by adjusting existing space–time code designs over frequency-selective MIMO channels to collect joint space–Doppler gains over purely time-selective MIMO channels. Further, [14] uses the ideas of [12] to develop a space–time code that can achieve full space-delay-Doppler diversity for any number of transmit–receive antennas. However, to quantify the maximum Doppler diversity order [2], the above papers rely on a parsimonious critically sampled complex-exponential basis expansion model (CCE-BEM) for the underlying purely time-selective or doubly-selective channels [16]. However, the CCE-BEM may have a large modeling error under certain channel conditions [17].

In this paper, we develop a novel STBC for multi-antenna transmissions over doubly-selective channels. The proposed STBC is designed for a multiple-input single-output (MISO) system with two transmit antennas and one receive antenna, i.e., a  $2 \times 1$  system, but the ideas can be extended to a general multiple-input multiple-output (MIMO) system. The proposed technique can be interpreted as the extension of the Alamouti code to doubly-selective channels, and relies on a joint time–frequency reversal of the transmitted sequences. Assuming a block fading channel where the time-variation from subblock to subblock is modeled by a CCE-BEM (we will label such a channel as a *block fading CCE-BEM channel*), the proposed STBC belongs to the class that achieves full spatial, delay, and Doppler diversity using a maximum-likelihood (ML) receiver, as well as a linear zero-forcing (LZF) or linear minimum mean-squared error (LMMSE) receiver. For realistic doubly-selective channels, which cannot exactly be modeled by a block fading CCE-BEM channel, a real-valued linear data model is presented, for which different receiver structures can be developed. In that case, the notion of Doppler diversity is difficult to define, but comparing the proposed STBC with existing approaches by simulation we notice great improvements. Note though that our STBC relies

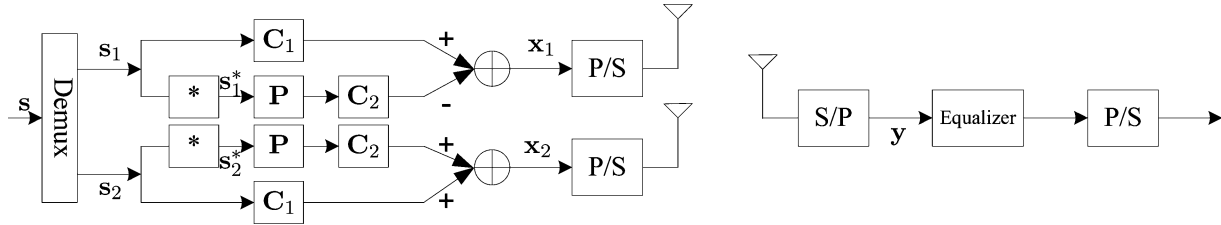


Fig. 1. System model of the proposed STBC system.

on the orthogonal structure of [5], which incurs a rate loss up to 50% when more than two transmit antennas and complex constellations are used. This paper assumes that the receiver has perfect channel state information (CSI), as well as perfect knowledge of the maximum delay spread  $\tau_{\max}$  and the maximum Doppler spread  $f_{\max}$  which can be derived from the wireless transmission channel. The transmitter on the other hand has no access to CSI.

*Notation:* We use upper (lower) bold face letters to denote matrices (column vectors).  $(\cdot)^*$ ,  $(\cdot)^T$ , and  $(\cdot)^H$  represent complex conjugate, transpose and complex conjugate transpose (Hermitian), respectively.  $E\{x\}$  stands for the expectation with respect to  $x$ .  $a \bmod b$  gives the remainder of  $a$  divided by  $b$ . We use  $[\mathbf{x}]_p$  to indicate the  $(p+1)$ st element of  $\mathbf{x}$ , and  $[\mathbf{X}]_{p,q}$  to indicate the  $(p+1, q+1)$ st entry of  $\mathbf{X}$ . Further, we let  $\mathbf{I}_N$  denote an  $N \times N$  identity matrix and  $\mathbf{0}_{M \times N}$  an  $M \times N$  all-zero matrix.  $\mathbf{F}_N$  denotes the unitary  $N$ -point DFT matrix with  $[\mathbf{F}_N]_{p,q} = 1/\sqrt{N}e^{-j2\pi/Npq}$ . We use the symbol  $\otimes$  to denote the Kronecker product between matrices. The  $J \times J$  permutation matrices  $\{\mathbf{P}_J^{(n)}\}_{n=0}^{J-1}$  are defined to perform a reversed cyclic shift, i.e.,  $[\mathbf{P}_J^{(n)}\mathbf{a}]_p = [\mathbf{a}]_{(J-p+n) \bmod J}$ .

## II. SYSTEM MODEL

For simplicity reasons, we consider a single-user MISO communication system with two transmit antennas and one receive antenna, i.e., a  $2 \times 1$  system, as shown in Fig. 1. However, the proposed methods can be easily adapted to a general MIMO system. More specifically, extensions to multiple transmit antennas can be obtained by following the generalizations of the Alamouti code to more than two transmit antennas, whereas extensions to multiple receive antennas can be realized by applying the proposed methods to a stack of the different receive antennas. We focus on a discrete-time baseband-equivalent description. Suppose  $x_t[n]$  is the symbol sequence transmitted over the  $t$ th transmit antenna. The received signal can then be written as

$$y[n] = \sum_{t=1}^2 \sum_{l=0}^L h_t[n; l] x_t[n-l] + \eta[n] \quad (1)$$

where  $h_t[n; l]$  is the order- $L$  time- and frequency-selective channel from the  $t$ th transmit antenna to the receive antenna, and  $\eta[n]$  is the additive noise. The channel order  $L$  depends on the channel delay spread and should be chosen to satisfy  $LT \geq \tau_{\max}$ , with  $T$  being the symbol period as well as the sampling period.

Suppose now that the STBC has a length of  $N$ . In order to avoid inter block interference (IBI), we design our STBC codewords in such a way that the last  $L$  symbols within each codeword are zero (as shown in the next section). Since IBI is then avoided, the equalizer at the receiver can be designed for each codeword separately. For simplicity reasons, we here focus on the first codeword; the other codewords can be treated in a similar fashion. Parsing  $x_t[n]$  and  $y[n]$  into blocks of length  $N$ , with  $\mathbf{x}_t = [x_t[0], x_t[1], \dots, x_t[N-1]]^T$  and  $\mathbf{y} = [y[0], y[1], \dots, y[N-1]]^T$ , respectively, the input-output relationship can be expressed as

$$\mathbf{y} = \sum_{t=1}^2 \mathbf{H}_t \mathbf{x}_t + \boldsymbol{\eta} \quad (2)$$

where  $\mathbf{H}_t$  is the  $N \times N$  channel matrix with  $[\mathbf{H}_t]_{n,n'} = h_t[n; (n-n') \bmod N]$  (we may use the modulo operator here since every codeword has  $L$  zeros at the end), and  $\boldsymbol{\eta} = [\eta[0], \eta[1], \dots, \eta[N-1]]^T$ . For simplicity, we assume that  $\boldsymbol{\eta}$  is a circular complex Gaussian noise vector with zero mean and covariance matrix  $E\{\boldsymbol{\eta}\boldsymbol{\eta}^H\} = \sigma_\eta^2 \mathbf{I}_N$ .

## III. SPACE-TIME BLOCK CODING

Orthogonal STBC [4], [5] has been designed to achieve the spatial diversity offered by multiple transmit and/or receive antennas. The STBC schemes proposed in [4] and [5] are designed for flat-fading channels, which lead to a performance degradation in time- and frequency-selective channels. Our goal is to design efficient STBC schemes to counteract the effects of doubly-selective channels. The basic idea of the proposed STBC for a  $2 \times 1$  system is to multiplex the data sequence in two data subsequences and to generate two orthogonal full-diversity subchannels over doubly-selective channels. Then, we apply a scheme that is similar to the Alamouti code. On the first antenna, we send the first data subsequence in the first subchannel and a negative permuted version of the complex conjugate of the second data subsequence in the second subchannel. On the second antenna, we send the second data subsequence in the first subchannel and a permuted version of the complex conjugate of the first data subsequence in the second subchannel. The questions that now remain are how we can generate two orthogonal full-diversity subchannels over doubly-selective channels, and how the permutations should look like in order to obtain a good performance. Both these questions can be answered by assuming a restrictive yet simple doubly-selective channel model. More specifically, we assume a *block fading CCE-BEM* channel, which is defined as a block fading channel where the time-variation from subblock to subblock is modeled by a CCE-BEM. Hence, we first develop and analyze the STBC under this block fading CCE-BEM channel model, and then, we show how to decode the STBC for real-life channels, which do not exactly fit this block fading CCE-BEM channel model.

### A. Block Fading CCE-BEM Channel Model

Let us start by defining what we exactly mean by a block fading CCE-BEM channel model. We assume that within the span of one STBC codeword, the doubly-selective channel behaves like a block fading channel, where the fading from subblock to subblock can be described by a CCE-BEM. Assume for instance that the span of the STBC codeword can be split into  $2P'$  subblocks of length  $K'$ , i.e.,  $N = 2P'K'$ . Every channel is then assumed to be constant within every subblock of length  $K'$  and to vary over the  $2P'$  subblocks as a CCE-BEM, which uses  $2Q+1$  complex exponential basis functions to model the time variation over the  $2P'$  subblocks

$$h_t[n; l] = \sum_{q=-Q}^Q e^{j2\pi(\lfloor n/K' \rfloor)q/(2P')} h_{t,q}[l] \quad (3)$$

where  $h_{t,q}[l]$  is the  $q$ th CCE-BEM coefficient of the  $l$ th channel tap within the STBC codeword. The  $(L+1)(2Q+1)$  BEM coefficients  $\{\{h_{t,q}[l]\}_{l=0}^L\}_{q=-Q}^Q$  remain constant during each length- $N$  block, and are allowed to change over different length- $N$  blocks. The  $2Q+1$  CCE-BEM basis functions used to capture the time variations are the

same for every length- $N$  block.  $Q$  can be regarded as the discrete Doppler spread index with frequency-domain resolution  $1/(NT)$ , and it needs to satisfy  $Q/(NT) \geq f_{\max}$ . Different from [2], [15], where the CCE-BEM is used to model the time-variation of the channel from sample to sample, we now use it to model the time-variation of the channel from subblock to subblock.

Under the block fading CCE-BEM channel model, the channel matrix  $\mathbf{H}_t$  from (2) can be written as

$$\mathbf{H}_t = \sum_{q=-Q}^Q (\mathbf{A}_{2P',q} \otimes \mathbf{I}_{K'}) \mathbf{H}_{N,t,q} \quad (4)$$

where  $\mathbf{A}_{2P',q}$  is the  $2P' \times 2P'$  diagonal matrix given by  $[\mathbf{A}_{2P',q}]_{p,p} = e^{j2\pi pq/(2P')}$  and  $\mathbf{H}_{N,t,q}$  is the  $N \times N$  circulant matrix given by  $[\mathbf{H}_{N,t,q}]_{n,n'} = h_{t,q}[(n - n') \bmod N]$ .

### B. Code Design

In [15], it has been shown how to generate orthogonal full-diversity subchannels in case the CCE-BEM is adopted to model the time-variation of the channel from sample to sample. More specifically, in [15], a multi-user communications scheme is developed where users remain orthogonal after propagation over a doubly-selective channel and where the full delay-Doppler diversity of a doubly-selective channel is enabled. Similarly, the same transmission scheme can be used to generate two orthogonal full-diversity subchannels in case the CCE-BEM is used to model the time-variation of the channel from subblock to subblock, i.e., in case we have a block fading CCE-BEM channel. This will be the basis of our STBC design.

Assuming  $K' > L$  and  $P' > 2Q$ , and defining  $K = K' - L$  and  $P = P' - 2Q$ , let us introduce the channel-independent  $N \times PK$  spreading matrices  $\mathbf{C}_u$  and  $N \times P'K'$  despreading matrices  $\mathbf{D}_u$  defined as [15]

$$\mathbf{C}_u = [\mathbf{F}_{2P'}^H(\mathbf{c}_u \otimes \mathbf{T}_2)] \otimes \mathbf{T}_1 \quad (5)$$

$$\mathbf{D}_u = [\mathbf{F}_{2P'}^H(\mathbf{c}_u \otimes \mathbf{I}_{P'})] \otimes \mathbf{I}_{K'} \quad (6)$$

where  $\mathbf{T}_1 = [\mathbf{I}_K, \mathbf{0}_{K \times L}]^T$  is the  $K' \times K$  zero padding matrix,  $\mathbf{T}_2 = [\mathbf{0}_{P \times Q}, \mathbf{I}_P, \mathbf{0}_{P \times Q}]^T$  is the  $P' \times P$  two-sided zero inserting matrix, and  $\{\mathbf{c}_u\}_{u=1}^2$  is an arbitrary set of two orthonormal code vectors. Notice that the last  $L$  rows of the spreading matrix  $\mathbf{C}_u$  are set to zero, which avoids the IBI. Similar to [15], it is possible to show that these spreading matrices  $\mathbf{C}_u$  and despreading matrices  $\mathbf{D}_u$  can be used to create two orthogonal full-diversity subchannels under the assumption of a block fading CCE-BEM channel model. The composite channel matrix consisting of the block fading CCE-BEM channel as well as the spreading and despreading operations can be expressed as [15]

$$\mathbf{D}_u^H \mathbf{H}_t \mathbf{C}_u = \begin{cases} \mathcal{H}_t \mathbf{T}, & u' = u; \\ \mathbf{0}_{P'K' \times PK}, & u' \neq u, \end{cases} \quad (7)$$

where  $\mathcal{H}_t = \sum_{q=-Q}^Q \mathbf{J}_{P',q} \otimes \mathbf{H}_{K',t,q}$  and  $\mathbf{T} = \mathbf{T}_2 \otimes \mathbf{T}_1$ , with  $\mathbf{J}_{P',q}$  the  $P' \times P'$  circulant matrix given by  $[\mathbf{J}_{P',q}]_{p,p'} = \delta[(p - p' - q) \bmod P']$  and  $\mathbf{H}_{K',t,q}$  the  $K' \times K'$  circulant matrix given by  $[\mathbf{H}_{K',t,q}]_{k,k'} = h_{t,q}[(k - k') \bmod K']$ .

The proposed STBC now proceeds as mentioned earlier. We start by demultiplexing a  $2PK \times 1$  data vector  $\mathbf{s}$  into two  $PK \times 1$  data subvectors  $\mathbf{s}_1$  and  $\mathbf{s}_2$ , where the data symbols are assumed to be circular complex with zero mean and covariance matrix  $\mathbb{E}\{\mathbf{s}\mathbf{s}^H\} = \sigma_s^2 \mathbf{I}_{2PK}$ . On the first and second antenna, we then send

$$\begin{aligned} \mathbf{x}_1 &= \mathbf{C}_1 \mathbf{s}_1 - \mathbf{C}_2 \mathbf{P} \mathbf{s}_2^* \\ \mathbf{x}_2 &= \mathbf{C}_1 \mathbf{s}_2 + \mathbf{C}_2 \mathbf{P} \mathbf{s}_1^* \end{aligned} \quad (8)$$

where  $\mathbf{P}$  is a  $PK \times PK$  permutation matrix that will be determined later on. The received signal can now be expressed as

$$\begin{aligned} \mathbf{y} &= \mathbf{H}_1 \mathbf{x}_1 + \mathbf{H}_2 \mathbf{x}_2 + \boldsymbol{\eta} \\ &= \mathbf{H}_1 \mathbf{C}_1 \mathbf{s}_1 - \mathbf{H}_1 \mathbf{C}_2 \mathbf{P} \mathbf{s}_2^* + \mathbf{H}_2 \mathbf{C}_1 \mathbf{s}_2 \\ &\quad + \mathbf{H}_2 \mathbf{C}_2 \mathbf{P} \mathbf{s}_1^* + \boldsymbol{\eta}. \end{aligned} \quad (9)$$

Applying the despreading operations  $\mathbf{D}_1$  and  $\mathbf{D}_2$  at the receiver, we obtain

$$\bar{\mathbf{y}}_1 = \mathbf{D}_1^H \mathbf{y} = \mathcal{H}_1 \mathbf{T} \mathbf{s}_1 + \mathcal{H}_2 \mathbf{T} \mathbf{s}_2 + \bar{\boldsymbol{\eta}}_1 \quad (10)$$

$$\bar{\mathbf{y}}_2 = \mathbf{D}_2^H \mathbf{y} = \mathcal{H}_2 \mathbf{T} \mathbf{P} \mathbf{s}_1^* - \mathcal{H}_1 \mathbf{T} \mathbf{P} \mathbf{s}_2^* + \bar{\boldsymbol{\eta}}_2. \quad (11)$$

Since the  $N \times P'K'$  despreading matrix  $\mathbf{D}_u$  is a tall matrix and  $\mathbf{D}_u^H \mathbf{D}_u = \mathbf{I}_{P'K'}$  [15],  $\bar{\boldsymbol{\eta}}_u$  is still a circular complex Gaussian noise vector with zero mean and covariance matrix  $\mathbb{E}\{\bar{\boldsymbol{\eta}}_u \bar{\boldsymbol{\eta}}_u^H\} = \sigma_{\bar{\boldsymbol{\eta}}}^2 \mathbf{I}_{P'K'}$ .

We wish to be able to decode the two multiplexed transmitted data streams  $\mathbf{s}_1$  and  $\mathbf{s}_2$  separately at the receiver, similar to the scalar case for Alamouti decoding [4]. In order to achieve that, we now have to find the  $PK \times PK$  permutation matrix  $\mathbf{P}$  such that there exists a  $P'K' \times P'K'$  permutation matrix  $\mathbf{P}'$  for which

$$\mathbf{P}' \mathcal{H}_t \mathbf{T} \mathbf{P} = \mathcal{H}_t^T \mathbf{T}. \quad (12)$$

Since  $\mathcal{H}_t$  is a block circulant matrix of circulant matrices, it is easy to show similar to [6] that the permutation matrices that satisfy this property are given by  $\mathbf{P} = \mathbf{P}_P^{(P-1)} \otimes \mathbf{P}_K^{(K-1)}$ , and  $\mathbf{P}' = \mathbf{P}_{P'}^{(P'-1)} \otimes \mathbf{P}_{K'}^{(K'-1)}$ . Note that  $\mathbf{P}$  actually represents a  $PK \times PK$  element reversal, where due to the structure of the spreading matrices, the first part ( $\mathbf{P}_P^{(P-1)}$ ) can be interpreted as a frequency reversal and the second part ( $\mathbf{P}_K^{(K-1)}$ ) as a time reversal. As a result, (11) can be rewritten as

$$\mathbf{P}' \bar{\mathbf{y}}_2^* = \mathcal{H}_2^H \mathbf{T} \mathbf{s}_1 - \mathcal{H}_1^H \mathbf{T} \mathbf{s}_2 + \mathbf{P}' \bar{\boldsymbol{\eta}}_2^*. \quad (13)$$

Now applying  $\mathbf{F} = \mathbf{F}_{P'} \otimes \mathbf{F}_{K'}$  to (10) and (13), we get

$$\mathbf{F} \bar{\mathbf{y}}_1 = \mathcal{G}_1 \mathbf{F} \mathbf{T} \mathbf{s}_1 + \mathcal{G}_2 \mathbf{F} \mathbf{T} \mathbf{s}_2 + \mathbf{F} \bar{\boldsymbol{\eta}}_1 \quad (14)$$

$$\mathbf{F} \mathbf{P}' \bar{\mathbf{y}}_2^* = \mathcal{G}_2^* \mathbf{F} \mathbf{T} \mathbf{s}_1 - \mathcal{G}_1^* \mathbf{F} \mathbf{T} \mathbf{s}_2 + \mathbf{F} \mathbf{P}' \bar{\boldsymbol{\eta}}_2^*. \quad (15)$$

In these formulas,  $\mathcal{G}_t = \mathbf{F} \mathcal{H}_t \mathbf{F}^H$  is a  $P'K' \times P'K'$  diagonal matrix. Stacking (14) and (15), we obtain the following relationship:

$$\begin{aligned} \tilde{\mathbf{y}} &= \begin{bmatrix} \mathbf{F} \bar{\mathbf{y}}_1 \\ \mathbf{F} \mathbf{P}' \bar{\mathbf{y}}_2^* \end{bmatrix} = \begin{bmatrix} \mathcal{G}_1 & \mathcal{G}_2 \\ \mathcal{G}_2^* & -\mathcal{G}_1^* \end{bmatrix} \begin{bmatrix} \mathbf{F} \mathbf{T} \mathbf{s}_1 \\ \mathbf{F} \mathbf{T} \mathbf{s}_2 \end{bmatrix} + \begin{bmatrix} \mathbf{F} \bar{\boldsymbol{\eta}}_1 \\ \mathbf{F} \mathbf{P}' \bar{\boldsymbol{\eta}}_2^* \end{bmatrix} \\ &= \mathcal{G} \begin{bmatrix} \mathbf{F} \mathbf{T} \mathbf{s}_1 \\ \mathbf{F} \mathbf{T} \mathbf{s}_2 \end{bmatrix} + \bar{\boldsymbol{\eta}}. \end{aligned} \quad (16)$$

Similar to [6], if we define  $\mathcal{G}_{12} = (\mathcal{G}_1^* \mathcal{G}_1 + \mathcal{G}_2^* \mathcal{G}_2)^{1/2}$  and apply the unitary matrix  $\mathbf{U} = \mathcal{G}(\mathbf{I}_2 \otimes \mathcal{G}_{12}^{-1})$ , we obtain

$$\mathbf{U}^H \tilde{\mathbf{y}} = \begin{bmatrix} \mathcal{G}_{12} \mathbf{F} \mathbf{T} \mathbf{s}_1 \\ \mathcal{G}_{12} \mathbf{F} \mathbf{T} \mathbf{s}_2 \end{bmatrix} + \mathbf{U}^H \bar{\boldsymbol{\eta}}. \quad (17)$$

Note that if  $\mathcal{G}_1$  and  $\mathcal{G}_2$  share a common zero, we can still design a unitary  $\mathbf{U}$  without compromising the validity of (17), by replacing either one of the common zeros by a one in the formula for  $\mathbf{U}$ , as explained in [6].

In conclusion, by applying complex conjugations and linear unitary matrix operations, we can separate the two substreams, leading to two matrix equations of the form

$$\mathbf{z}_u = \mathcal{G}_{12} \mathbf{F} \mathbf{T} \mathbf{s}_u + \zeta_u = \mathbf{H} \mathbf{s}_u + \zeta_u \quad (18)$$

where  $\mathbf{z}_u$  ( $\zeta_u$ ) represents the corresponding part of  $\mathbf{U}^H \tilde{\mathbf{y}}$  ( $\mathbf{U}^H \bar{\boldsymbol{\eta}}$ ) in (17). Every stream can then be decoded using your favorite decoder.

Note that all these derivations only hold under the assumption of a block fading CCE-BEM channel model.

### C. Diversity Gain Analysis

Similar to [2], [15], we can show that if a (near-)ML decoder is used, the delay-Doppler diversity order of  $(2Q + 1)(L + 1)$ , which is the number of degrees of freedom in the block fading CCE-BEM channel, can be reached, under the assumption that the CCE-BEM coefficients are independently zero-mean complex Gaussian distributed. Alamouti-like STBC offers an additional spatial diversity order of 2. Hence, the proposed STBC enables the maximum space-delay-Doppler diversity that the doubly-selective channel can offer, which is multiplicative in the degrees of freedom of the channel in space, time and frequency dimensions. The proof is an extension of those in [2], [15], and we only give a brief description here.

Since each data stream can be decoded separately in (18), we consider decoding  $\mathbf{z}_1$  only. Define the error vector  $\mathbf{e} = \mathbf{s}_1 - \mathbf{s}'_1$  between symbol blocks  $\mathbf{s}_1$  and  $\mathbf{s}'_1$ . The squared Euclidean distance between  $\mathbf{z}_1 = \mathbf{H}\mathbf{s}_1$  and  $\mathbf{z}'_1 = \mathbf{H}\mathbf{s}'_1$  can then be expressed as

$$d^2(\mathbf{z}_1, \mathbf{z}'_1) = \|\mathbf{H}\mathbf{e}\|^2. \quad (19)$$

In [2] and [15], it is shown that maximum space-delay-Doppler diversity can be achieved if  $\mathbf{H}$  has full column rank  $PK$ , which is proved in Appendix A.

Using the results of [18], we can even show that if a LZFB or LMMSE decoder is used, this full diversity order can still be achieved. In a general context, it is shown in [18] that if  $\det(\mathbf{H}^H\mathbf{H}) > 0$ ,  $\forall \mathbf{H}$ , i.e.,  $\mathbf{H}$  has full column rank for any channel realization, then the LZFB and LMMSE decoder can obtain the same diversity order as the ML decoder.

### D. Proposed Receiver for Realistic Channels

The STBC design and analysis discussed before is based on the block fading CCE-BEM channel model. The nice algebraic structure of this block fading CCE-BEM channel model allows us to extend the Alamouti code to doubly-selective channels enabling the full space-delay-Doppler diversity, as shown in Section III-B. Although this channel model was useful to design and analyze our STBC, it does not perfectly model real-life doubly-selective channels under all circumstances [17]. Hence, the receiver processing discussed in Section III-B can only be applied if we approximate the true channel by its best possible fit to a block fading CCE-BEM channel. The related modeling error will of course introduce a bit-error-rate (BER) performance floor at medium to high signal-to-noise ratio (SNR), and this floor will increase with the Doppler spread. To avoid this floor, we will next propose an alternative receiver for the proposed STBC that is suitable for realistic doubly-selective channels, which do not rely on any specific channel model, so that there is no channel modeling error.

First of all, we realize that in case of a block fading CCE-BEM channel, working with  $\mathbf{z} = [\mathbf{z}_1^T, \mathbf{z}_2^T]^T$  [see (18)] is the same as working with  $\tilde{\mathbf{z}} = [\Re\{\mathbf{z}^T\}, \Im\{\mathbf{z}^T\}]^T$ , since the data and noise are circular complex white. Further, it is easy to understand that working with  $\tilde{\mathbf{z}}$  is also the same as working with  $\tilde{\mathbf{y}}$ , since  $\mathbf{z}$  is obtained from  $\mathbf{y}$  by applying complex conjugations and unitary matrix operations which has no effect on the receiver performance if the noise and the data are circular complex white [19]. This shows that any receiver (ML, LZFB, or LMMSE) applied to  $\mathbf{z}$  would have the same performance as when we would apply a similar receiver to  $\tilde{\mathbf{y}}$  in case of a block fading CCE-BEM channel. The advantage of designing a receiver for  $\tilde{\mathbf{y}}$  however is that it can be generalized to realistic doubly-selective channels that do not

necessarily fit into the block fading CCE-BEM channel model. To design such a receiver, we have to develop a data model for  $\tilde{\mathbf{y}}$ , which will be a real-valued data model.

Defining the  $N \times PK$  matrix  $\mathbf{K}_{t,u}$  as  $\mathbf{K}_{t,u} = \mathbf{H}_t\mathbf{C}_u$ , the received vector  $\mathbf{y}$  can be written as

$$\mathbf{y} = \mathbf{K}_{1,1}\mathbf{s}_1 - \mathbf{K}_{1,2}\mathbf{P}\mathbf{s}_2^* + \mathbf{K}_{2,1}\mathbf{s}_2 + \mathbf{K}_{2,2}\mathbf{P}\mathbf{s}_1^* + \boldsymbol{\eta}. \quad (20)$$

Further defining

$$\tilde{\mathbf{K}}_{t,u} = \begin{bmatrix} \Re(\mathbf{K}_{t,u}) & -\Im(\mathbf{K}_{t,u}) \\ \Im(\mathbf{K}_{t,u}) & \Re(\mathbf{K}_{t,u}) \end{bmatrix}, \quad (21)$$

$$\tilde{\tilde{\mathbf{K}}}_{t,u} = \begin{bmatrix} \Re(\mathbf{K}_{t,u}) & \Im(\mathbf{K}_{t,u}) \\ \Im(\mathbf{K}_{t,u}) & -\Re(\mathbf{K}_{t,u}) \end{bmatrix} \quad (22)$$

we can write  $\tilde{\mathbf{y}}$  as

$$\begin{aligned} \tilde{\mathbf{y}} &= \tilde{\mathbf{K}}_{1,1}\tilde{\mathbf{s}}_1 - \tilde{\tilde{\mathbf{K}}}_{1,2}(\mathbf{I}_2 \otimes \mathbf{P})\tilde{\mathbf{s}}_2 + \tilde{\mathbf{K}}_{2,1}\tilde{\mathbf{s}}_2 + \tilde{\tilde{\mathbf{K}}}_{2,2}(\mathbf{I}_2 \otimes \mathbf{P})\tilde{\mathbf{s}}_1 + \tilde{\boldsymbol{\eta}} \\ &= [\tilde{\mathbf{K}}_{1,1} + \tilde{\tilde{\mathbf{K}}}_{2,2}(\mathbf{I}_2 \otimes \mathbf{P}) \quad \tilde{\mathbf{K}}_{2,1} - \tilde{\tilde{\mathbf{K}}}_{1,2}(\mathbf{I}_2 \otimes \mathbf{P})] \begin{bmatrix} \tilde{\mathbf{s}}_1 \\ \tilde{\mathbf{s}}_2 \end{bmatrix} + \tilde{\boldsymbol{\eta}} \\ &= \tilde{\mathbf{K}}\tilde{\mathbf{s}} + \tilde{\boldsymbol{\eta}}. \end{aligned} \quad (23)$$

On this real-valued data model, one can then apply any decoder, from a (near-)ML decoder to a LZFB or LMMSE decoder. In this paper, we only consider the LMMSE decoder, and the estimated transformed symbol sequence is then given by

$$\hat{\tilde{\mathbf{s}}} = \tilde{\mathbf{K}}^H \left( \tilde{\mathbf{K}}\tilde{\mathbf{K}}^H + \frac{\sigma_s^2}{\sigma_n^2} \mathbf{I}_{2N} \right)^{-1} \tilde{\mathbf{y}}. \quad (24)$$

From  $\hat{\tilde{\mathbf{s}}}$ , the original transmitted symbols can be recovered.

## IV. SIMULATION RESULTS

In this section, the proposed STBC is examined and compared with other coding schemes by simulations. We only consider a system with two transmit antennas and one receive antenna. The maximum channel delay spread is set to  $L = 2$ . The channel taps from each transmit antenna to the receive antenna are independent and identically distributed (i.i.d.) circular complex Gaussian distributed with zero mean and variance  $E\{|h_t[n, l]|^2\} = 1/(L + 1)$  (i.e., uniform power delay profile) and they follow Jakes' Doppler profile. Quaternary phase-shift keying (QPSK) symbols with energy  $\sigma_s^2$  are used for transmission. The two orthonormal code vectors are set to  $\mathbf{c}_1 = [1/\sqrt{2}, 1/\sqrt{2}]^T$  and  $\mathbf{c}_2 = [1/\sqrt{2}, -1/\sqrt{2}]^T$ , which are the columns of the  $2 \times 2$  unitary Hadamard matrix. The SNR is defined as  $\sigma_s^2/\sigma_n^2$ . The normalized Doppler spread is defined as  $f_d = v f/cT$ , where  $v$  denotes the mobile velocity,  $f$  is the carrier frequency, and  $c$  is the speed of light. The receiver applies the LMMSE decoder of (24), unless explicitly defined otherwise.

1) *Test Case 1:* We first compare the BER performance of the proposed STBC applying the LMMSE decoder of (24), with the performance in case we approximate the true channel by the best possible block fading CCE-BEM channel and adopt the receiver processing of Section III-B. We consider large normalized Doppler spreads so that the block fading CCE-BEM cannot model the time-varying channel very well, in order to show the necessity of the real-valued linear data model. We especially focus on the achievable Doppler diversity order for different Doppler spreads. The symbol block lengths in the frequency and time domain are set to  $P = 14$  and  $K = 7$ , respectively. Fig. 2 shows the BER performance of a system with normalized Doppler spread  $f_d = 0.002$ . It can be shown that a frequency domain guard band of  $Q = 1$  is enough to suppress the interference

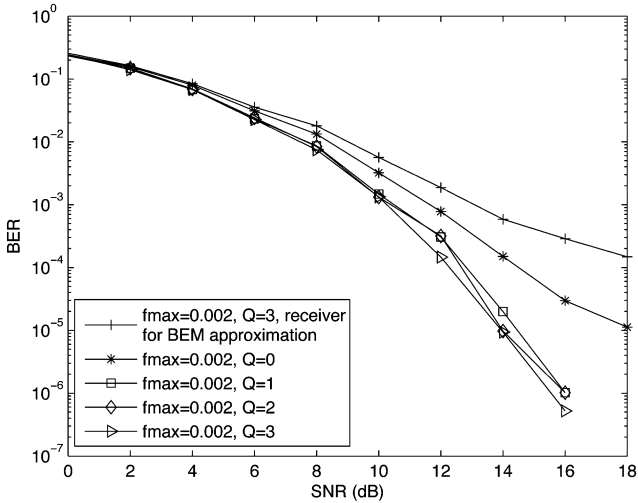


Fig. 2. BER performance with normalized Doppler spread  $f_d = 0.002$ .

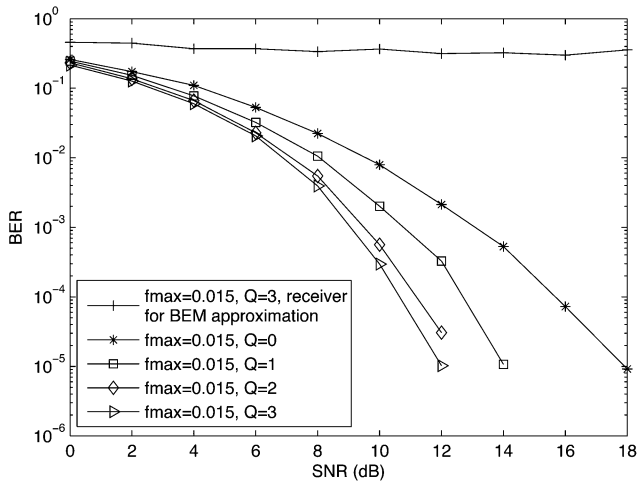


Fig. 3. BER performance with normalized Doppler spread  $f_d = 0.015$ .

due to the time-varying channel effects. However, when the approximate block fading CCE-BEM channel is considered, we observe an error floor even with  $Q = 3$  due to the channel modeling error. In Fig. 3, the normalized Doppler spread is increased to  $f_d = 0.015$ . The simulation result shows that a larger  $Q$  is required, as increasing  $Q$  leads to a better BER performance. Meanwhile, higher Doppler spreads lead to a lower BER because the Doppler diversity increases as the Doppler spread increases. On the other hand, when the approximate block fading CCE-BEM channel is considered, the receiver completely fails since it cannot model such a rapidly time-varying channel. Notice that as we increase  $Q$ , the block length  $N$  increases and the spectral efficiency decreases.

2) *Test Case 2:* We next compare the proposed STBC with the DPS algorithm of [14] for doubly-selective channels. The symbol block lengths are set to  $P = 27$  and  $K = 8$ . The frequency domain guard band length is set to  $Q = 3$ , which is large enough for the Doppler spread used in this simulation, for both approaches. The spectral efficiency of the proposed STBC is  $\varepsilon = 0.65$ , which is higher than the spectral efficiency of DPS  $\varepsilon_{\text{DPS}} = 0.54$ , meaning that we disfavor our approach. We use the LMMSE decoder for both algorithms. It is clearly shown in Fig. 4 that the proposed STBC can achieve a better BER performance due to a larger coding gain. The diversity order is almost the same for both approaches, which increases as the Doppler spread increases.

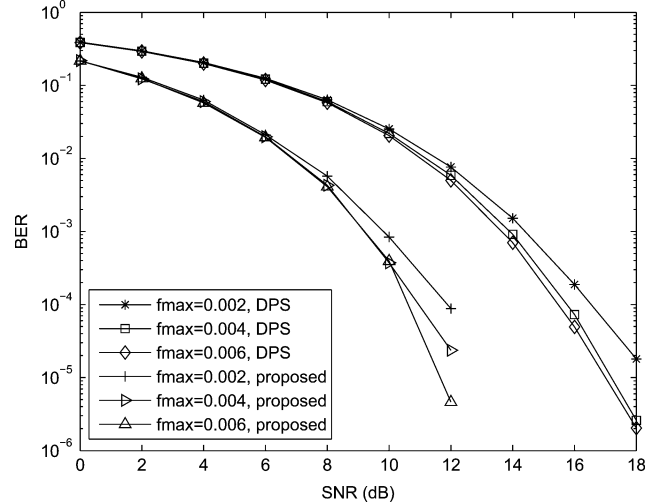


Fig. 4. BER comparison of proposed STBC with DPS [14].

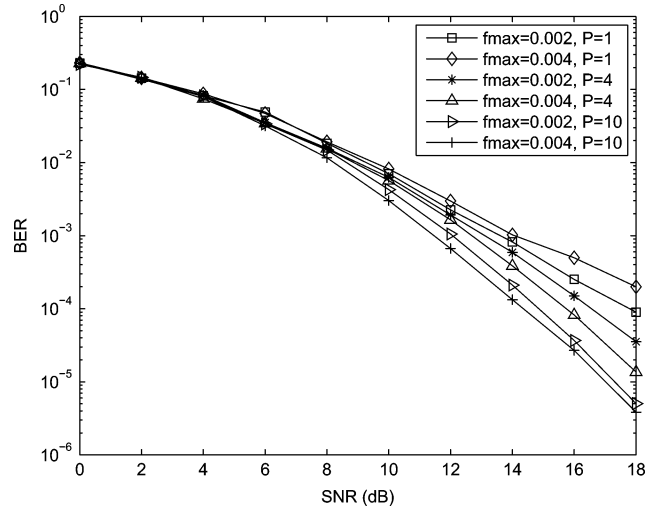


Fig. 5. BER comparison of proposed STBC with the STBC of [6] (case  $P = 1$ ).

3) *Test Case 3:* Finally, we compare the proposed STBC with the STBC designed for frequency-selective channels in [6]. The zero-padding only STBC in [6] can actually be regarded as a special case of the proposed STBC with  $P = 1$  and  $Q = 0$ . Without data symbol spreading and guards in the frequency domain ( $P = 1, Q = 0$ ), a higher spectral efficiency can be achieved, and the block length can be made smaller, which also leads to a lower complexity. A natural question is then if we can ignore the time-selectivity and only use the STBCs designed for a frequency-selective channel in doubly-selective channels. To have the same spectral efficiency, we set  $Q = 0$  for the proposed STBC, and keep  $K = 5$  fixed for both approaches. Since [6] considers a purely frequency-selective channel, the decoder of [6] relies on the fact that the channel is constant during the entire space-time codeword. To obtain a fair comparison, we simulate the approach of [6] by using our LMMSE receiver, with  $P = 1$  and  $Q = 0$ , so that the STBC design is the same as in [6], but the receiver does not require the channel to be constant. The simulation results in Fig. 5 show that we get a better BER performance as we increase  $P$ . But the BER performance is worse compared to the  $Q > 0$  case shown in Fig. 4. This is due to the interference related to the lack of frequency-domain guard bands. However, Doppler diversity can still be explored even without a frequency-domain guard band. As shown in the figure, when  $P = 1$ , i.e., when the data symbols are only spread

in the time domain, a higher Doppler spread leads to a worse BER performance. When  $P > 1$ , a higher Doppler spread leads to a better BER performance, and as  $P$  increases, the BER becomes smaller due to an increasing Doppler diversity.

## V. CONCLUSION

We have developed a novel STBC for multi-antenna transmissions over doubly-selective channels. By spreading the data symbols in the space–time–frequency dimensions with appropriate guard bands, the proposed STBC can achieve the full spatial, delay, and Doppler diversity, using the ML receiver as well as using a LZF or LMMSE receiver, under a specific channel model. Further, a real-valued linear data model has been presented for realistic doubly-selective channels, for which different receiver structures can be developed. Simulation results have shown significantly improved performance by jointly exploring the space–delay–Doppler diversity in doubly-selective channels.

## APPENDIX

### PROOF OF FULL COLUMN RANK $PK$ FOR $\mathbf{H}$

The compound channel matrix  $\mathbf{H}$  can be expressed as

$$\mathbf{H} = \mathcal{G}_{12} \mathbf{F} \mathbf{T} \\ = (\mathcal{G}_1^* \mathcal{G}_1 + \mathcal{G}_2^* \mathcal{G}_2)^{1/2} (\mathbf{F}_{P'} \mathbf{T}_2 \otimes \mathbf{F}_{K'} \mathbf{T}_1) \quad (25)$$

where  $\mathcal{G}_t$  is a  $P'K' \times P'K'$  diagonal matrix. We define  $\mathcal{G}_t = \text{diag}(\mathbf{V}_{1,t}, \dots, \mathbf{V}_{P',t})$ , where  $\mathbf{V}_{k,t}$  is a  $K' \times K'$  diagonal matrix. By stacking the diagonal elements of  $\mathcal{G}_t$  in a  $P' \times K'$  matrix  $\mathbf{V}_t$ , we can rewrite  $\mathcal{G}_t = \mathbf{F} \mathbf{H}_t \mathbf{F}^H$  as

$$\mathbf{V}_t = \mathbf{B} \mathbf{G}_t \quad (26)$$

where the  $k$ th row of  $\mathbf{V}_t$  contains the diagonal elements of  $\mathbf{V}_{k,t}$ , and  $\mathbf{B}$ , and  $\mathbf{G}_t$  are, respectively, a  $P' \times (2Q+1)$  matrix and a  $(2Q+1) \times K'$  matrix given by

$$\mathbf{B} = \begin{pmatrix} 1 & \cdots & 1 & \cdots & 1 \\ \alpha^{-Q} & \cdots & 1 & \cdots & \alpha^Q \\ \vdots & \ddots & \vdots & \ddots & \vdots \\ \alpha^{-(P'-1)Q} & \cdots & 1 & \cdots & \alpha^{(P'-1)Q} \end{pmatrix}, \quad (27)$$

$$\mathbf{G}_t = \begin{pmatrix} H_{t,-Q}[1] & \cdots & H_{t,-Q}[K'] \\ \vdots & \ddots & \vdots \\ H_{t,Q}[1] & \cdots & H_{t,Q}[K'] \end{pmatrix} \quad (28)$$

where  $\alpha = e^{j2\pi/P'}$ , and  $H_{t,q}[k] = [\mathbf{F}_{K'}^H \mathbf{H}_{K',t,q} \mathbf{F}_{K'}^H]_{k,k}$ . Since the elements of the  $q$ th row of  $\mathbf{G}_t$  are the  $K'$ -point frequency response of  $h_{t,q}[l]$ , and an order- $L$  polynomial has at most  $L$  roots, it is easy to show that each row of  $\mathbf{G}_t$  either contains at most  $L$  zeros, or is a full-zero row in case  $\{h_{t,q}[l]\}_{l=0}^{L-1} = 0$ . This means there are at most  $L$  full-zero columns in  $\mathbf{V}_t$ , which occurs when each nonzero row of  $\mathbf{G}_t$  has  $L$  zeros and they are located at the same position. Similarly, since an order- $2Q$  polynomial has at most  $2Q$  roots, and  $\mathbf{B}$  is a scaled  $P' \times (2Q+1)$  Vandermonde matrix, there are at most  $2Q$  zeros in each of the nonzero columns of the matrix  $\mathbf{V}_t$ . Finally, when  $\mathcal{G}_1$  and  $\mathcal{G}_2$  have zero elements at the same location, the corresponding elements of  $\mathcal{G}_{12}$  will be equal to zero.

We consider the case where  $\mathcal{G}_{12}$  has the maximum number of zeros, i.e., there are  $L$  full-zero columns in  $\mathbf{V}_t$ , and the remaining  $K$  columns

of  $\mathbf{V}_t$  all have  $2Q$  zeros. For the zero elements in the diagonal matrix  $\mathcal{G}_{12}$ , the corresponding rows of the matrix  $\mathbf{F}_{P'} \mathbf{T}_2 \otimes \mathbf{F}_{K'} \mathbf{T}_1$  can be set to zero. Suppose that  $\bar{\mathbf{P}}$  is a properly chosen permutation matrix that will group all the nonzero elements of  $\mathcal{G}_{12}$  at the top of the diagonal, then we can write (25) as

$$\mathbf{H} = \bar{\mathbf{P}} \bar{\mathbf{H}} \quad (29)$$

where

$$\bar{\mathbf{H}} = \begin{pmatrix} \bar{\mathcal{G}}_{12} \bar{\mathbf{F}}_{PK} \\ \mathbf{0}_{(P'L+2QK) \times PK} \end{pmatrix}. \quad (30)$$

Here, the  $PK \times PK$  diagonal matrix  $\bar{\mathcal{G}}_{12}$  contains the nonzero elements of  $\mathcal{G}_{12}$ , and

$$\bar{\mathbf{F}}_{PK} = \begin{pmatrix} \mathbf{f}_K^1 \otimes \mathbf{F}_P^1 \\ \mathbf{f}_K^2 \otimes \mathbf{F}_P^2 \\ \vdots \\ \mathbf{f}_K^K \otimes \mathbf{F}_P^K \end{pmatrix} \quad (31)$$

with  $\{\mathbf{f}_K^k\}_{k=1}^K$  the corresponding  $K$  nonzero rows of the matrix  $\mathbf{F}_{K'} \mathbf{T}_1$ , and  $\{\mathbf{F}_P^k\}_{k=1}^K$  the  $P \times P$  matrices containing the corresponding nonzero rows of the matrix  $\mathbf{F}_{P'} \mathbf{T}_2$ . It can be shown that the only solution of  $\bar{\mathbf{F}}_{PK}^T \mathbf{x} = \mathbf{0}$  is  $\mathbf{x} = \mathbf{0}$ , due to the Vandermonde structure of the matrices  $\mathbf{F}_{K'} \mathbf{T}_1$  and  $\mathbf{F}_{P'} \mathbf{T}_2$ , which means that the rows of the matrix  $\bar{\mathbf{F}}_{PK}$  are independent. As  $\bar{\mathbf{F}}_{PK}$  is a  $PK \times PK$  square matrix,  $\bar{\mathbf{F}}_{PK}$  thus has full rank  $PK$ . Since left-multiplying with a nonsingular matrix does not change the rank of the original matrix, we can conclude that the composite channel matrix  $\bar{\mathbf{H}}$  and thus  $\mathbf{H}$  are full column rank matrices when  $\mathcal{G}_{12}$  has the maximum number of zeros.

When  $\mathcal{G}_{12}$  has less zeros on the diagonal, and thus more rows of the matrix  $\mathbf{F}_{P'} \mathbf{T}_2 \otimes \mathbf{F}_{K'} \mathbf{T}_1$  are included, the column rank of  $\mathbf{H}$  will not reduce. Hence,  $\mathbf{H}$  has full column rank  $PK$  for all  $\mathbf{h} \neq \mathbf{0}$ . This concludes the proof.

## REFERENCES

- [1] A. M. Sayeed and B. Aazhang, "Joint multipath-Doppler diversity in mobile wireless communications," *IEEE Trans. Commun.*, vol. 47, no. 1, pp. 123–132, Jan. 1999.
- [2] X. Ma and G. B. Giannakis, "Maximum-diversity transmissions over doubly selective wireless channels," *IEEE Trans. Inf. Theory*, vol. 49, no. 7, pp. 1832–1840, Jul. 2003.
- [3] L. Zheng and D. N. C. Tse, "Diversity and multiplexing: A fundamental tradeoff in multiple antenna channels," *IEEE Trans. Inf. Theory*, vol. 49, no. 5, pp. 1073–1096, May 2003.
- [4] S. M. Alamouti, "A simple transmit diversity technique for wireless communications," *IEEE J. Sel. Areas Commun.*, vol. 16, no. 8, pp. 1451–1458, Oct. 1998.
- [5] V. Tarokh, H. Jafarkhani, and A. R. Calderbank, "Space-time block codes from orthogonal designs," *IEEE Trans. Inf. Theory*, vol. 45, no. 7, pp. 1456–1467, Jul. 1999.
- [6] S. Zhou and G. B. Giannakis, "Single-carrier space-time block coded transmissions over frequency-selective fading channels," *IEEE Trans. Inf. Theory*, vol. 49, no. 1, pp. 164–179, Jan. 2003.
- [7] E. Lindskog and A. Paulraj, "A transmit diversity scheme for channels with intersymbol interference," in *Proc. IEEE Int. Conf. Commun. (ICC)*, New Orleans, Jun. 2000, pp. 307–311.
- [8] N. Al-Dhahir, "Single-carrier frequency-domain equalization for space time block-coded transmissions over frequency-selective fading channels," *IEEE Commun. Lett.*, vol. 5, no. 7, pp. 304–306, Jul. 2001.

- [9] H. Bölcskei and A. J. Paulraj, "Space–frequency coded broadband OFDM systems," in *Proc. Wireless Commun. Netw. Conf. (WCNC)*, Chicago, IL, Sep. 2000, pp. 1–6.
- [10] H. Bölcskei and A. J. Paulraj, "Space–frequency codes for broadband fading channels," in *Proc. IEEE Int. Symp. Inf. Theory (ISIT)*, Washington, DC, Jun. 2001, p. 219.
- [11] Z. Liu, Y. Xin, and G. B. Giannakis, "Space–time–frequency coded OFDM over frequency-selective fading channels," *IEEE Trans. Signal Process.*, vol. 50, no. 10, pp. 2465–2476, Oct. 2002.
- [12] X. Ma and G. B. Giannakis, "Space–time–multipath coding using digital phase sweeping or circular delay diversity," *IEEE Trans. Signal Process.*, vol. 53, no. 3, pp. 1121–1130, Mar. 2005.
- [13] X. Ma, G. Leus, and G. B. Giannakis, "Space–time–Doppler block coding for correlated time-selective fading channels," *IEEE Trans. Signal Process.*, vol. 53, no. 6, pp. 2167–2181, Jun. 2005.
- [14] X. Ma and G. B. Giannakis, "Space–time coding for doubly selective channels," in *Proc. Int. Symp. Circuits Syst. (ISCAS)*, May 2002, vol. 3, pp. 647–650.
- [15] G. Leus, S. Zhou, and G. B. Giannakis, "Orthogonal multiple access over time- and frequency-selective channels," *IEEE Trans. Inf. Theory*, vol. 49, no. 8, pp. 1942–1950, Aug. 2003.
- [16] G. B. Giannakis and C. Tepedelenlioglu, "Basis expansion models and diversity techniques for blind identification and equalization of time-varying channels," *Proc. IEEE*, vol. 86, no. 10, pp. 1969–1986, Oct. 1998.
- [17] T. Zemen and C. F. Mecklenbraüker, "Time-variant channel estimation using discrete prolate spheroidal sequences," *IEEE Trans. Signal Process.*, vol. 53, no. 9, pp. 3597–3607, Sep. 2005.
- [18] X. Ma and W. Zhang, "Fundamental limits of linear equalizers: Diversity, capacity and complexity," *IEEE Trans. Inf. Theory*, vol. 54, no. 8, pp. 3442–3456, Aug. 2008.
- [19] B. Picinbono, "On circularity," *IEEE Trans. Signal Process.*, vol. 42, no. 12, pp. 3473–3482, Dec. 1994.

## DILAND: An Algorithm for Distributed Sensor Localization With Noisy Distance Measurements

Usman A. Khan, Soumya Kar, and José M. F. Moura

**Abstract**—We present an algorithm for distributed sensor localization with noisy distance measurements (DILAND) that extends and makes the DLRE more robust. DLRE is a distributed sensor localization algorithm in  $\mathbb{R}^m$  ( $m \geq 1$ ) introduced in our previous work (*IEEE Trans. Signal Process.*, vol. 57, no. 5, pp. 2000–2016, May 2009). DILAND operates when: 1) the communication among the sensors is noisy; 2) the communication links in the network may fail with a nonzero probability; and 3) the measurements performed to compute distances among the sensors are corrupted with noise. The sensors (which do not know their locations) lie in the convex hull of at least  $m + 1$  anchors (nodes that know their own locations). Under minimal assumptions on the connectivity and triangulation of each sensor in the network, we show that, under the broad random phenomena described above, DILAND converges almost surely (a.s.) to the exact sensor locations.

**Index Terms**—Absorbing Markov chain, anchor, barycentric coordinates, Cayley–Menger determinant, distributed iterative sensor localization, sensor networks, stochastic approximation.

### I. INTRODUCTION

Localization is an important problem in sensor networks, not only in its own right, but often as the first step toward solving more complicated and diverse network tasks, which may include environment monitoring, intrusion detection, and routing in geographically distributed communication networks. The problem we consider is when a large number of sensors do not know their locations, only a very few of them know their own. In [1], we presented a distributed sensor localization (DILOC) algorithm in  $\mathbb{R}^m$  ( $m \geq 1$ ), when we can divide the  $N$  nodes in the sensor network into these two sets: the set  $\kappa$  of  $n$  anchors, where  $n \geq m + 1$ , and the set  $\Omega$  of  $M$  sensors, with typically  $N \gg n$ . The  $n$  anchors are the nodes that know their exact locations, whereas the  $M$  sensors are the nodes that do not know their locations.<sup>1</sup> We assume that the sensors lie in the convex hull of the anchors, i.e.,  $\mathcal{C}(\Omega) \subset \mathcal{C}(\kappa)$ , where  $\mathcal{C}(\cdot)$  denotes the convex hull.<sup>2</sup> To each sensor  $l$  in the network, we associate

---

Manuscript received May 09, 2009; accepted November 19, 2009. First published December 11, 2009; current version published February 10, 2010. The associate editor coordinating the review of this manuscript and approving its publication was Prof. Hongbin Li. This work was supported in part by the NSF under grants ECS-0225449 and CNS-0428404 and by the ONR under grant MURI-N000140710747.

U. A. Khan was with the Department of Electrical and Computer Engineering, Carnegie Mellon University, Pittsburgh, PA 15213 USA. He is now with the Department of Electrical and Systems Engineering, University of Pennsylvania, Philadelphia, PA 19104 USA (e-mail: khanu@seas.upenn.edu).

S. Kar and J. M. F. Moura are with the Department of Electrical and Computer Engineering, Carnegie Mellon University, Pittsburgh, PA 15213 USA (e-mail: soumyyak@ece.cmu.edu; moura@ece.cmu.edu).

Color versions of one or more of the figures in this correspondence are available online at <http://ieeexplore.ieee.org>.

Digital Object Identifier 10.1109/TSP.2009.2038423

<sup>1</sup>In the sequel, we always use this disambiguation for sensors and anchors. When the statement is true for both sensors and anchors, we use the term *node*.

<sup>2</sup>The minimal number of anchors required for a nontrivial convex hull in  $m$ -dimensional ( $m$ D) space is  $m + 1$  that is a triangle in 2D space. We may have more than  $m + 1$  anchors forming the boundary of a polygon for less stringent requirements on sensor placement; see [2] for details.